JOURNAL OF Materials CHEMISTRY

Considerations of defect equilibria in high temperature proton-conducting cerates

Nikolaos Bonanos* and Finn Willy Poulsen

Materials Research Department, Risø National Laboratory, DK-4000, Roskilde, Denmark.
E-mail: nikolaos.bonanos@risoe.dk; finn.willy.poulsen@risoe.dk

Received 3rd July 1998, Accepted 10th November 1998

Acceptor doped perovskites such as strontium cerate form a variety of point defects through reaction with surrounding gases at high temperature, namely protons by dissolution of water vapour, electron holes by dissolution of oxygen and electrons by loss of oxygen. The defect equilibria can be described by three equilibrium constants coupled with electroneutrality and site conservation constraints. This work describes a numerical solution of these equations for arbitrary oxygen and water vapour partial pressures, without the need to neglect minority defects. It further examines the charge compensation mechanisms that dominate under the different regimes and their implications for transport properties.

1 Introduction

1.1 Background

Doped alkaline earth cerate and zirconate perovskites exhibit proton conduction at elevated temperatures[1–4] due to dissolution of water vapour and the formation of mobile protons. In such systems, an equilibrium arises between four types of point defects, namely oxide ion vacancies, protons, electrons and electron holes. The defect equilibria have been described for both vanishing[4,5] and finite[6,7] concentrations of free electrons, but these treatments have not taken into account a constraint namely, that of conservation of oxygen sites.

The present work describes a numerical solution of the complete set of defect equations, including this constraint. The solutions, presented in the form of two- and three-dimensional graphs of defect concentrations *versus* water vapour and oxygen partial pressures, are used to illustrate the dominant transport properties under various conditions and acceptor dopant concentrations. In common with earlier work,[4–7] this treatment ignores the Schottky defect equilibrium for which, in any case, the equilibrium constant is not available. The errors resulting from this omission will be negligible for heavily doped systems at temperatures low in comparison to their melting point, namely for typical perovskite proton conductors such as $SrCe_{0.95}Yb_{0.05}O_{2.975}$ or $BaCe_{0.90}Yb_{0.10}O_{2.95}$ at temperatures of 1200 °C or lower.

1.2 Definition of defect equilibria

Consider a system $AB_{1-y}M_yO_{3-y/2\pm\delta}$ where A and B are parent cations of valence 2 and 4 respectively and M is a trivalent cation substituting on the B-site. The following point defects and normal lattice oxygen are defined using the Kröger-Vink notation.[8]

Substitutional cation: M_B'

Oxide ion vacancy: $V_O^{\cdot\cdot}$

Proton (interstitial): $H_i^{\cdot}$

Electron hole: $h_i^{\cdot}$

Electron: e'

Normal oxygen $O_O^{\times}$

We now consider the following three defect reactions with their associated equilibrium equations. Dissolution of water vapour, with the generation of protons:

$$H_2O + V_O^{\cdot\cdot} \rightarrow O_O^{\times} + 2\ H_i^{\cdot} \quad (1a)$$

$$[H_i^{\cdot}]^2 = K_H\ P_{H_2O}\ [V_O^{\cdot\cdot}]\ [O_O^{\times}]^{-1} \quad (1b)$$

Dissolution of oxygen, with the generation of electron holes:

$$1/2\ O_2 + V_O^{\cdot\cdot} \rightarrow O_O^{\times} + 2\ h_i^{\cdot} \quad (2a)$$

$$[h_i^{\cdot}]^2 = K_h\ P_{O_2}^{1/2}\ [V_O^{\cdot\cdot}]\ [O_O^{\times}]^{-1} \quad (2b)$$

Loss of oxygen, at low partial pressure, with the generation of electrons:

$$O_O^{\times} \rightarrow V_O^{\cdot\cdot} + 2\ e' + 1/2\ O_2 \quad (3a)$$

$$[e']^2 = K_e\ P_{O_2}^{-1/2}\ [O_O^{\times}]\ [V_O^{\cdot\cdot}]^{-1} \quad (3b)$$

The above defect concentrations must satisfy the electroneutrality condition, namely:

$$2\ [V_O^{\cdot\cdot}] + [H_i^{\cdot}] + [h_i^{\cdot}] - [e'] - [M_B'] = 0 \quad (4)$$

and also the anion site conservation condition, which for a perovskite is as follows:

$$[V_O^{\cdot\cdot}] + [O_O^{\times}] = 3 \quad (5)$$

In the above, P_{H_2O} and P_{O_2} are independent variables, $[M_B']$, K_H, K_h and K_e are system and temperature dependent parameters and $[V_O^{\cdot\cdot}]$, $[H_i^{\cdot}]$, $[h_i^{\cdot}]$ and $[e']$ are the required solutions. The exciton equilibrium equation $[e'][h_i^{\cdot}] = K_{ex}$ is not explicitly used, but is implicit in the above, since it can be derived by multiplication of eqn. (2b) and (3b). In another formulation,[6] where the exciton equilibrium is included, (3b) is omitted. The above set of defect equations, and indeed more complex defect schemes involving cation vacancies, can be solved using an alternative, stepwise method proposed recently.[9] This uses the mathematical device of treating $[V_O^{\cdot\cdot}]$ as an independent variable and P_{O_2} as a dependent variable. As a result, however, that method cannot provide solutions at predefined values of oxygen partial pressure, leading to difficulties in the presentation of three-dimensional surface plots.

1.3 Solution of the analytical defect equation

Combining eqn. (5) with (1), (2) and (3) consecutively and taking square roots gives:

$$[H_i^{\cdot}] = K_H^{1/2}\ P_{H_2O}^{1/2}\ x \quad (6)$$

$$[h_i^{\cdot}] = K_h^{1/2}\ P_{O_2}^{1/4}\ x \quad (7)$$

$$[e'] = K_e^{1/2}\ P_{O_2}^{-1/4}\ x^{-1} \quad (8)$$

$$\text{where } x \equiv \{[V_O^{\cdot\cdot}]/(3 - [V_O^{\cdot\cdot}])\}^{1/2} \quad (9)$$

$$\text{in which case: } [V_O^{\cdot\cdot}] = (3x^2)/(x^2+1) \quad (10)$$

inserting eqn. (6)–(8) into the electroneutrality eqn. (4) and rearranging, yields:

$$\beta\, x^4 + (6 - [M_B'])\, x^3 + (\beta - \alpha)\, x^2 - [M_B']\, x - \alpha = 0 \quad (11)$$

$$\text{in which } \alpha \equiv K_e^{1/2} P_{O_2}{}^{-1/4} \quad (12)$$

$$\text{and } \beta \equiv K_H^{1/2} P_{H_2O}^{1/2} + K_h^{1/2}\, P_{O_2}{}^{1/4} \quad (13)$$

After solving eqn. (11), x is inserted into eqn. (6)–(8) and (10) to give the required defect concentrations. Eqn. (11) is quartic and, therefore, has an analytic solution, but, in practice it was found easier to implement a Newton–Raphson iterative solution, see for example ref. 10. If eqn. (11) is written in the form $f(x)=0$, the Newton–Raphson formula (14) gives the $(i+1)$th iteration of x in terms of the ith iteration.

$$x_{i+1} = x_i - f(x_i)/f'(x_i) \quad (14)$$

$$\text{where } f(x) = \beta\, x^4 + (6 - [M_B'])\, x^3 + (\beta - \alpha)\, x^2 - [M_B']\, x - \alpha \quad (15)$$

$$\text{and } f'(x) = 4\beta\, x^3 + 3(6 - [M_B'])\, x^2 + 2(\beta - \alpha)\, x - [M_B'] \quad (16)$$

The initial guess for x was provided by solving a quadratic equation (17) obtained under the assumptions $[e']=0$ and $x \ll 1$, the latter assumption allowing eqn. (10) to be simplified to $[V_O^{\cdot\cdot}] = 3x^2$.

$$6\, x^2 + \beta\, x - [M_B'] = 0 \quad (17)$$

$$\text{thus } x = \{-\beta + (\beta^2 + 24\, [M_B'])^{1/2}\}/12 \quad (18)$$

This solution is an excellent approximation for the full quartic model in the high-P_{O_2} regime, where the electron concentration is indeed negligible and the oxygen vacancy concentration never exceeds $[M_B']/2$. By using this initial guess, convergence was obtained within about ten iterations. To be on the safe side, fifteen iterations were used and the self-consistency of all solutions was checked by verifying electroneutrality.

2.3 Choice of simulation inputs

The purpose of this work is to focus on an interesting set of conditions, *i.e.* where several defects coexist in non-negligible concentrations. Therefore, wide ranges of partial pressure were chosen without concern as to their physical realisability, namely 10^{-8}–10^{8} atm for P_{H_2O} and 10^{-30}–10^{10} atm for P_{O_2}. The input parameters for the model are given in Table 1. For some typical perovskite proton conductors, values of K_H are available from thermogravimetric studies (Table 2), so K_H was assigned a realistic value for a rare earth doped cerate perovskite at 600–800 °C. Equilibrium constants K_h and K_e were set to values consistent, within about an order of magnitude, with those used by other authors.[7] The doping level, $[M_B']$, was held constant at 0.10, unless otherwise stated.

3 Results and discussion

The calculated concentrations for the four defects of interest are shown in Fig. 1(a) as a Brouwer diagram for a fixed P_{H_2O} of 10^{-2} atm. Over a wide range of P_{O_2}, the ionic defects (oxide ion vacancies and protons) have constant concentrations: $[V_O^{\cdot\cdot}]=0.028$; $[H_i^{\cdot}]=0.044$, corresponding to a water uptake of almost half the saturation value. The electronic defects behave as minority carriers. As shown in Fig. 1(b), the electroneutrality errors in these calculations are consistently 10^{-16} or less and are no doubt the result of rounding off errors in the calculation of x.

Fig. 2 shows the same defect concentrations as three-dimensional plots calculated for a logarithmically spaced grid of P_{O_2} and P_{H_2O}. In certain partial pressure ranges, the oxide ion vacancy and proton concentrations have plateaus which may be associated with intrinsic compensation regimes. For oxide ion vacancies [Fig. 2(a)] the plateau occurs at $[V_O^{\cdot\cdot}]=0.05$, determined by the simplified electroneutrality condition $2[V_O^{\cdot\cdot}] \approx [M_B']$. The latter limit is valid for very low proton uptake, *i.e.* very low water partial pressures. For the protons the plateau occurs at $[H_i^{\cdot}] \approx 0.10$, corresponding to the condition $[H_i^{\cdot}] \approx [M_B']$. These regimes are well understood and experimentally accessible in real systems. For the holes, a plateau corresponding to $[h_i^{\cdot}] \approx [M_B']$ was expected at very high P_{O_2}, but this was not found in the parameter space covered. Instead, the hole concentration increased monotonically with increasing P_{O_2} and decreasing P_{H_2O} [Fig. 2(c)]. For the acceptor doped system modelled, no intrinsic compensation regime is expected for electrons and indeed their concentration increases monotonically with increasing P_{H_2O} and decreasing P_{O_2} [Fig. 2(d)]. Outside the extrinsic regimes, more complex compensation conditions apply. When both P_{H_2O} and P_{O_2} are low, the vacancy concentration rises according to the condition $2[V_O^{\cdot\cdot}] \approx [M_B'] + [e']$. Conversely, at low P_{H_2O} and high P_{O_2}, oxygen is dissolved in the solid and the vacancy concentration

Table 1 Input parameters used for the simulation study

Description	Symbol	Value
Doping level for trivalent ion on B-site	$[M_B']$	0.10[a]
Equilibrium constant for proton formation	K_H	20 atm^{-1}
Equilibrium constant for hole formation	K_h	10^{-5} $atm^{-1/2}$
Equilibrium constant for electron formation	K_e	10^{-17} $atm^{1/2}$

[a]Valid for all simulations except those shown in Fig. 3, in which $[M_B']$ has been varied.

Table 2 Experimental equilibrium constant K_H for selected perovskite proton conductors[a]

Compound	T/°C	K_H/atm^{-1}	Ref.
$BaCe_{0.95}Gd_{0.05}O_{2.975}$	600	26	11
$BaCe_{0.95}Nd_{0.05}O_{2.975}$	600	13	12
$BaCe_{0.95}Nd_{0.05}O_{2.975}$	900	3	12
$(Ba_{0.98}Gd_{0.02})(Ce_{0.87}Gd_{0.13})O_{2.945}$	800	20[b]	13

[a]The original literature values were based on models defining $[O_O^{\times}] \leqslant 1$. To reconcile these with the present site conservation equation, according to which $[O_O^{\times}] \leqslant 3$, the quoted literature values have been multiplied by a factor of 3. [b]Single crystal material; value interpolated from data supplied by authors.

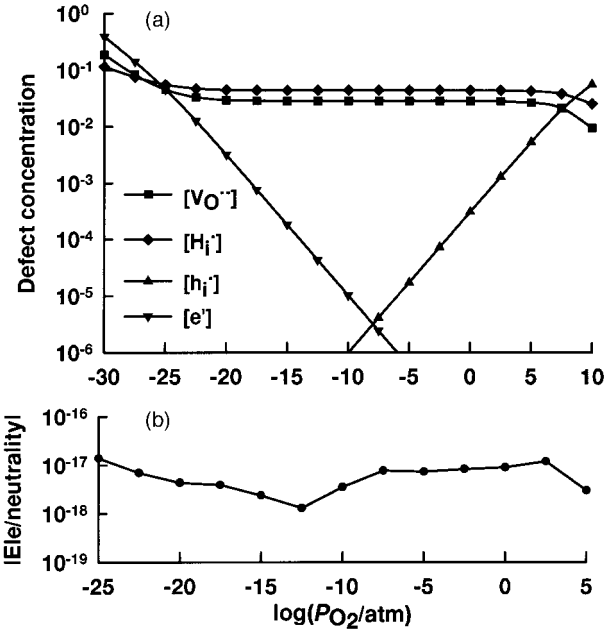

Fig. 1 (a) Brouwer diagram of defect concentrations in a perovskite proton conductor for the case $[M_B']=0.1$ and $P_{H_2O}=10^{-2}$ atm. (b) Electroneutrality errors for the calculations.

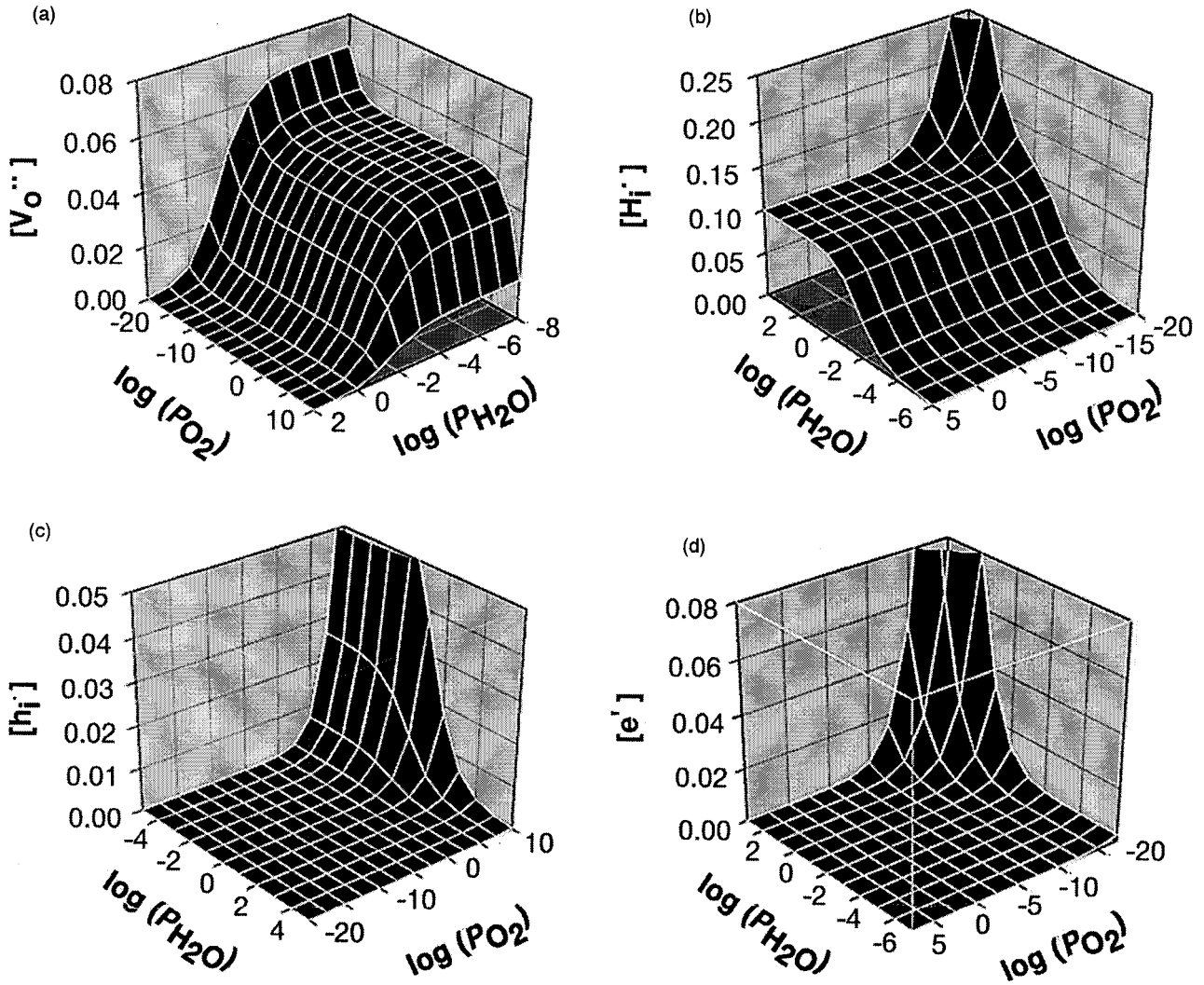

Fig. 2 Defect concentrations for a logarithmically spaced grid of P_{O_2} and P_{H_2O} for the case $[M_B']=0.1$. (a) oxide ion vacancies, (b) protons, (c) holes and (d) electrons. Partial pressures are in atm. The plateaus visible in (a) and (b) correspond to intrinsic charge compensation regimes.

falls, a situation that may be described by the condition $2[V_O^{\cdot\cdot}]+[h_i^{\cdot}]\approx[M_B']$.

Fig. 3 shows the four defect concentrations of interest as a function of dopant concentration for a fixed water vapour pressure of 10^{-2} atm. For vacancies and protons [Fig. 3(a)] and for holes [Fig. 3(b)] the calculations were performed for $P_{O_2}=1$ atm and for electrons [Fig. 3(c)] for $P_{O_2}=10^{-20}$ atm. As shown in Fig. 3(a), the concentrations of the ionic defects have different curvatures and $[V_O^{\cdot\cdot}]$ and $[H_i^{\cdot}]$ cross over at $[M_B']=0.20$, as well as in the trivial case $[M_B']=0$. It is interesting that for the realistic value of K_H used, the quantity $[H_i^{\cdot}]-[V_O^{\cdot\cdot}]$ is maximum at $[M_B']=0.075$; *i.e.* at this doping level protons dominate most strongly over vacancies. This may be linked to the empirical fact that, in this type of compound, pure protonic conductivity is achieved at doping levels of around 5%.[1–4] The concentrations of vacancies and protons are almost independent of the equilibrium constants K_h and K_e, provided these are both much lower than K_H, as is the case in the present simulations.

The electronic defects behave as expected but, in view of the uncertainty over K_h and K_e, their main use here is for showing qualitative trends. Thus $[h_i^{\cdot}]$ increases with doping level [Fig. 3(b)] in a manner similar to $[H_i^{\cdot}]$. As shown in Fig. 3(c), calculated for low oxygen partial pressure conditions, the electron concentration decreases with acceptor doping.

Fig.4 shows the P_{O_2} dependence of [e′] and $[H_i^{\cdot}]$, for the case $[M_B']=0.1$ and $P_{H_2O}=10^{-2}$ atm. For most of the simulated P_{O_2} range, electrons are minority carriers and [e′] is proportional to $(P_{O_2})^{-0.25}$ [Fig. 4(a)] and $[H_i^{\cdot}]$ is constant [Fig. 4(b)]. However, at $P_{O_2}<10^{-20}$ atm, the slope of log([e′]) *versus* $\log(P_{O_2})$ begins to fall and $[H_i^{\cdot}]$ increases rapidly. Inspection of the output data files for this regime indicated an effective electroneutrality condition $2[V_O^{\cdot\cdot}]+[H_i^{\cdot}]-[e']-[M_B'']\approx 0$. Over the whole P_{O_2} range, the data in Fig. 4(b) is described by the power law $[H_i^{\cdot}]=a+b(P_{O_2})^{-0.15}$. Assuming a constant proton mobility, in these circumstances, the protonic conductivity would have an oxygen partial pressure dependence that might suggest that it is *n*-type electronic. This effect, which, to the authors' knowledge has not been pointed out before, might explain some discrepancies in the reported conduction mechanisms of proton conducting perovskites, as discussed below.

Acceptor doped $SrCeO_3$ and $BaCeO_3$ have been described as partial *n*-type electronic conductors due to an increase in conductivity at low partial pressures of oxygen.[14–16] On the other hand, in hydrogen-rich atmospheres, these compounds are found to retain high protonic transport numbers, as demonstrated by their ability to pump hydrogen electrochemically.[15] The above simulations show that, under strongly reducing conditions, the concentrations of protons and electrons can both be significant. Which carrier dominates the conductivity will depend on the relative magnitude of their mobilities; obviously, if the electrons had a much lower mobility, the protons would dominate. Therefore, a reliable identification of the conduction mechanism cannot be made

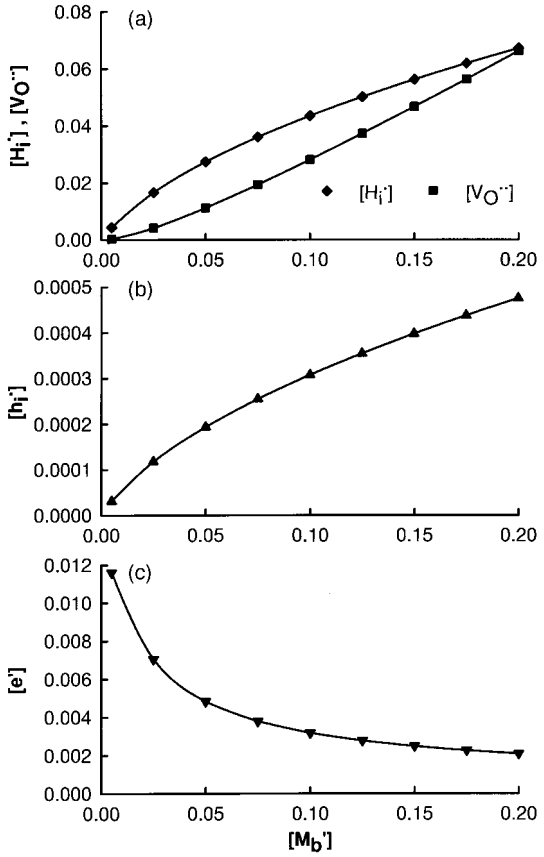

Fig. 3 Defect concentrations in a perovskite proton conductor as a function of acceptor dopant concentration calculated for a fixed P_{H_2O} of 10^{-2} atm. (a) Oxide ion vacancies and protons for $P_{O_2}=1$ atm; (b) holes for $P_{O_2}=1$ atm; (c) electrons for $P_{O_2}=10^{-20}$ atm.

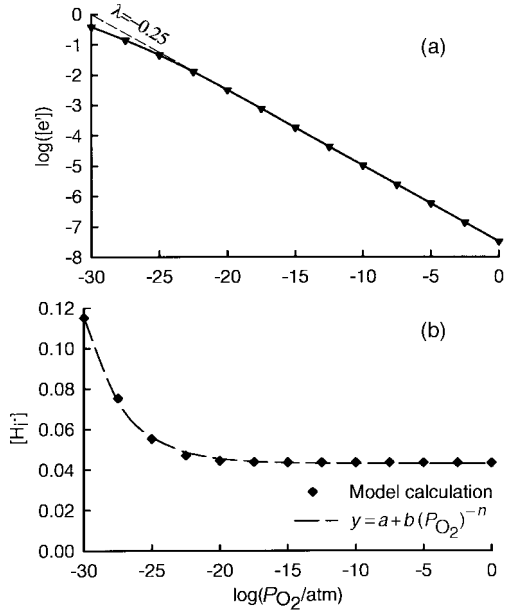

Fig. 4 Oxygen partial pressure dependence of the concentrations of (a) electrons and (b) protons in a perovskite proton conductor for $[M_B']=0.1$ and $P_{H_2O}=10^{-2}$ atm. At $P_{O_2}<10^{-20}$ atm the slope $\log([e'])$ *versus* $\log(P_{O_2})$ changes. Over the whole range, the concentration of protons follows a power law, plotted as a solid line.

on the basis of conductivity alone, but should be supplemented by electrochemical determinations, such as concentration cells studies or the faradaic transport of oxygen and/or hydrogen.

If the temperature dependence of the equilibrium constants is known, the above solution can be easily applied to thermogravimetric data; the sample weight can be calculated from the oxygen stoichiometry, $3-[V_O^{\cdot\cdot}]$, and proton concentration. It can also be used to model the total conductivities, provided the mobilities of the charge carriers are known. Considering the iterative nature of the solution, it is difficult to imagine using the full model to obtain equilibrium constants by fitting to conductivity data, but approximate solutions, such as the quadratic one described, can and have been used, see for example ref. 5.

4 Conclusions

The concentration of ionic and electronic defects in a perovskite proton conductor was obtained by numerical solution of a quartic equation involving three equilibrium constants, the doping level and the partial pressures of water vapour and oxygen. In certain ranges of partial pressure, the concentrations of vacancies and protons follow simple electroneutrality conditions such as $2[V_O^{\cdot\cdot}]\approx[M_B']$ or $[h^{\cdot}]\approx[M_B']$, corresponding to extrinsic doping regimes. Simulation of the low oxygen partial pressure regime shows that the protonic concentration varies with P_{O_2}, potentially giving rise to confusion with *n*-type electronic conductivity. The total electrical conductivity can be modelled if the charge carrier mobilities are known.

5 Acknowledgements

Yang Du and K.-D. Kreuer are acknowledged for supplying data on water vapour equilibrium constants, M. Mogensen, T. Norby and B. C. H. Steele are thanked for useful discussions and B. Zachau-Christiansen is thanked for a critical reading of the manuscript. This work was supported by the Materials Research Department, under the fundamental Defect Chemistry project and by the New Energy Development Organisation (NEDO) of Japan under the project *Advanced Ceramics for Protonics*, led by Professor H. Iwahara.

References

1 H. Iwahara, T. Esaka, H. Uchida and N. Maeda, *Solid State Ionics*, 1981, **3/4**, 359.
2 H. Iwahara, Proc. Intl. Conference on advanced materials (ICAM 91), Symposium A2: Solid State Ionics, Strasbourg, 27–31 May 1991, Ed. M. Balkanski, T. Takahashi and H. L. Tuller, Intl. Union of Materials Research Societies, Amsterdam, 1992, 575.
3 H. Iwahara, *Advanced Ceramics for Protonics*, in *High Temperature Electrochemistry*, *Ceramics and Metals*, Proc. 17th Risø Intl. Symposium on Materials Science, ed. F. W. Poulsen, N. Bonanos, S. Linderoth, M. Mogenson and B. Zachau-Christiansen, Risø National Laboratory, Roskilde, Denmark, 1996, Sept. 2–6.
4 H. Uchida, H. Yoshikawa and H. Iwahara, *Solid State Ionics*, 1989, **35**, 229.
5 Y. Larring and T. Norby, *Solid State Ionics*, 1997, **97**, 523.
6 T. Schober and H. Wenzl, *Ionics*, 1995, **81**, 111.
7 T. Schober, W. Schilling and H. Wenzl, *Solid State Ionics*, 1996, **86–88**, 653.
8 F. A. Kröger, and H. J. Vink, *Solid State Physics*, ed. F. Seitz and D. Turnbull, Academic Press, New York, vol. 3, pp. 307–435.
9 F. W. Poulsen, *J. Solid State Chem.*, 1999, in press.
10 S. Barnet and T. M. Cronin, *Mathematical Formulae for Engineering and Science Students*, Bradford University Press, 1971, p. 45.
11 J. F. Liu and A. S. Nowick, *Solid State Ionics*, 1992, **50**, 131.
12 A. S. Nowick and Du. Yang, *Solid State Ionics*, 1995, **77**, 137.
13 K-D. Kreuer, Th. Dippel, Yu. M. Baikov and J. Maier, *Solid State Ionics*, 1996, **86–88**, 613.
14 N. Bonanos, *J. Phys. Chem. Solids*, 1993, **54**, 867.
15 I. Kosacki and H. L Tuller, *Solid State Ionics*, 1995, **80**, 223.
16 E. O. Ahlgren, J. R. Hansen, N. Bonanos, F. W. Poulsen and M. Mogensen, *Electrical characterisation of* $SrCe_{0.95}Y_{0.05}O_{3-\delta}$, in *High Temperature Electrochemistry*, *Ceramics and Metals*, Proc. 17th Risø Intl. Symposium on Materials Science, ed. F. W. Poulsen, N. Bonanos, S. Linderoth, M. Mogenson and B. Zachau-Christiansen, Risø National Laboratory, Roskilde, Denmark, 1996, Sept. 2–6.

Paper 8/05150J